Physics/Dynamics Coupling

Sylvie Malardel

ECMWF, Shinfield Park, Reading
RG2 9AX, United Kingdom
Sylvie.Malardel@ecmwf.int

1 Introduction

In an atmospheric model, the dynamics computes the "resolved" and adiabatic terms of the equations. The physics computes the diabatic (including latent heat release and microphysics) and the mean subgrid scale effects.

This numerical separation between the "adiabatic" model and the "diabatic" parametrisations is such that the evolution of air parcels is computed as an adiabatic transformation (in the dynamics) "modified" by local diabatic tendencies.

The current design of the coupling between the IFS dynamics and physics follows hypotheses which are valid for the hydrostatic model. These hypotheses have to be reexamined for the coupling of the non-hydrostatic (NH) core with a physics package. It needs to be checked in particular that the physics/NH dynamics interface respects the basic conservation principles.The coherence between the hypotheses inside the parametrisations and the adiabatic NH equations must also be analysed.

2 Physics/Dynamics coupling for the NH IFS system of equations

2.1 Adiabatic thermodynamics equations in the NH IFS

In the non-hydrostatic fully compressible dynamical core of the IFS, the prognostic thermodynamic parameters are the temperature T and a parameter $\hat{q}$ derived from the true pressure p (Bubnova et al., 1995, Wedi et al., 2008)

$$\hat{q} = \ln(\frac{p}{\pi})$$

π is the hydrostatic part of the pressure[1] defined by $\partial\pi/\partial z = -\rho g$, where ρ is the "true" density.

In the NH dynamics, the evolution of the temperature[2] is given by the thermodynamics equation initially written as an equation for the internal energy of air parcels

$$\frac{D_{\mathscr{D}}(T)}{Dt} = -\frac{1}{c_v} RTD_3 \tag{1}$$

[1] In the NH model, the hydrostatic pressure is defined as the pressure which would be necessary for the pressure gradient force to be in balance with gravity. This parameter describes the mass field rather than the pressure field. In the NH range of processes, the hydrostatic pressure π describes a mass field which is not a solution of "true" hydrostatic balance nor gives the pressure field what the flow converges to when adjusting to the hydrostatic equilibrium.

[2] $\frac{D_{\mathscr{D}}}{Dt}$ represents the total evolution in the dynamics, including the advection by the resolved motion.

where D_3 is the 3D divergence. In a fully compressible system, D_3 is linked to the evolution of the "true" density

$$D_3 = -\frac{1}{\rho}\frac{D_{\mathscr{D}}(\rho)}{Dt}$$

In the NH-IFS, the T-equation is coupled with an equation for $\hat{q}$ obtained from combining the perfect gas law and the continuity equation

$$\frac{D_{\mathscr{D}}(\hat{q})}{Dt} = -\frac{c_p}{c_v}D_3 - \frac{\omega}{\pi} \tag{2}$$

where $\omega = D_{\mathscr{D}}(\pi)/Dt$[3].

Combining equation (2) and equation (1) gives the enthalpy form of the thermodynamics equation:

$$\frac{D_{\mathscr{D}}(T)}{Dt} = \frac{RT}{c_p}\left[\frac{D_{\mathscr{D}}(\hat{q})}{Dt} + \frac{\omega}{\pi}\right] = \frac{RT}{c_p}\frac{1}{p}\frac{D_{\mathscr{D}}(p)}{Dt} \tag{3}$$

This equation is used in the hydrostatic core of the IFS, but in this case $p = \pi$ and $\hat{q} = 0$.

2.2 Fully compressible diabatic equations for the NH pressure departure

The resolved 3D motions and transports are computed in the dynamics. Therefore, the physics tendencies are computed as "local" tendencies in the physics. The parametrisations are not allowed to modify the "resolved" mass distribution (no resolved motion in the physics). The physics tendencies are then computed for a "frozen" mass distribution. The dynamical "solver" computes later the resolved 3D motions of the air and the associated mass re-organisation in agreement with the dynamical core equations.

The current parametrisations of the IFS are designed following these hypotheses. All the computations are performed for a given mass (at contant hydrostatic pressure) in a given grid box (it is assumed that the mass does not move).

We note D/Dt the total derivative of a parameter in a time step. D/Dt is the sum of the adiabatic evolution $D_{\mathscr{D}}/Dt$ and a local physical tendency $\partial_\varphi/\partial t$.

In the NH model, even if the mass (hydrostatic pressure) is still not supposed to be modified in the physics parametrisations, the NH pressure is a new degree of freedom.

In the continuous equations of the NH model, the diabatic equation for the pressure departure $\hat{q}$ is :

$$\frac{D(\hat{q})}{Dt} = \left(\frac{D_{\mathscr{D}}(\hat{q})}{Dt} + \frac{\partial_\varphi(\hat{q})}{\partial t}\right) = -\frac{c_p}{c_v}D_3 - \frac{\omega}{\pi} + \frac{Q}{c_v T} \tag{4}$$

where Q is the diabatic heating. In this equation, Q is a source/sink of NH pressure departure.

In a literal application of equation (4), the non-hydrostatic pressure departure should be updated by the diabatic tendencies computed in the physics.

[3]By definition, π gives a description of the mass field rather than a description of the pressure field. ω then gives an indication about the evolution of the mass distribution in the atmosphere. In the NH model, the description of the mass (hydrostatic pressure) evolution given by ω may be non hydrostatic (in this case, ω decribes the evolution of the mass field of a flow which is not in balance with the pressure gradient force field).

2.3 Fully compressible diabatic equations for the temperature

The diabatic form of the internal energy equation used in the NH core of the IFS is:

$$\frac{D(T)}{Dt} = \left(\frac{D_{\mathscr{D}}(T)}{Dt} + \frac{\partial_{\varphi}(T)}{\partial t} \right) = -\frac{1}{c_v} RTD_3 + \frac{Q}{c_v} \tag{5}$$

In a literal coding of equation (5), the physics should return Q/c_v in the NH IFS.

A physics/dynamics coupling which directly follows the continuous equations (5) and (4) should then update the temperature with parametrised tendencies in agreement with the contribution of the T-evolution already computed in the dynamics by an internal energy form of the thermodynamics equation. It should also update the NH pressure departure.

2.4 Physics/dynamics coupling with the current IFS interface

The current parametrisations of the IFS have been developed for the hydrostatic model. They are based on transformations at constant (hydrostatic) pressure. They do not produce any tendency for the true pressure and they return a T-tendency computed as Q/c_p in agreement with the enthalpy form of the thermodynamics equation used in the hydrostatic model.

If the current physics/dynamics interface is used in the NH dynamical model, the evolution of T and $\hat{q}$ is given by the following system:

$$\frac{D(\hat{T})}{Dt} = \left(\frac{D_{\mathscr{D}}(T)}{Dt} + \frac{\partial_{\varphi}(T)}{\partial t} \right) = -\frac{RT}{c_v} D_3 + \frac{Q}{c_p} \tag{6}$$

$$\frac{D(\hat{q})}{Dt} = \frac{D_{\mathscr{D}}(\hat{q})}{Dt} = -\frac{c_p}{c_v} D_3 - \frac{\omega}{\pi} \tag{7}$$

This system contains an approximation which was shown by Thurre (1998) to filter the accoustic waves generated by physics forcings. This approximation is called *anelastic coupling* and it is investigated in the following sections.

The coupling between the dynamics and the physics was also modified in order to restore equations (5) and (4). The T-tendency coming from the physics is multiplied by c_p/c_v and the NH pressure departure is updated following equations (4). The results obtained with this modified coupling (called *compressible coupling*) are compared to the solution obtained with the anelastic coupling and to the solution given by the hydrostatic model.

3 Validation in the hydrostatic range

In this section, the results given by the hydrostatic model are compared to the results obtained with the non-hydrostatic model with "anelastic" coupling and the non-hydrostatic model with "compressible" coupling for a 10 day forecast with a T255 spectral truncation (equivalent to a resolution of about 125 km near the equator).

At such a low resolution, the hydrostatic model and the non-hydrostatic models should give quasi-identical results.

The geopotential and temperature at 500hPa of the different simulations are compared to the analysis. RMS errors are shown in figure (1).

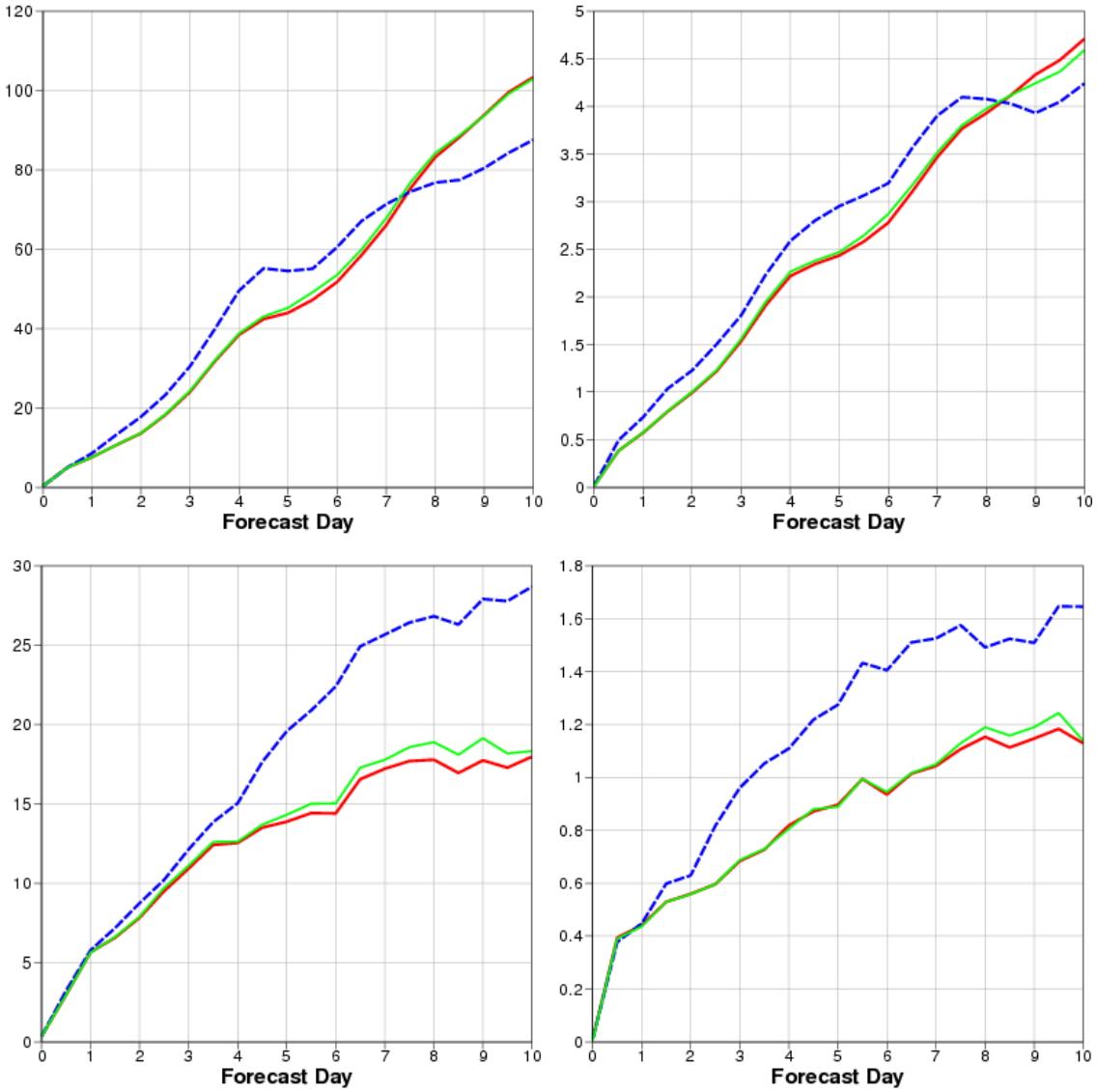

Figure 1: RMS error of 500 hPa geopotential (left) and temperature (right). Top: North hemisphere (lat>20N), bottom: tropics. Results for anelastic coupling (red curve), compressible coupling (blue curve) and hydrostatic (green curve).

The NH forecast with anelastic coupling and the hydrostatic forecast give very similar results. But the NH forecast with compressible coupling is significantly different. The differences are largest in the tropics. A carefull analysis of the results shows that the convective systems are much weaker than in the hydrostatic forecast.

At resolutions in the hydrostatic range, the NH core coupled with the current physics and the current "anelastic" coupling and the hydrostatic model give almost identical solutions. However, the T-tendencies computed in the current physics with the current sequential organisation of the time step are not compatible with a "naive" modification of the physics/dynamics coupling which aims at restoring the fully compressible equations.

4 Validation in the NH range

The IFS cannot yet be run on the real globe at a resolution in the NH range. However, the NH system can already be tested at high resolution on a planet with a "reduced" radius and with academic test cases (Wedi et al., 2008).

The sensitivity studies presented in the two following sections are carried out on such a planet with a radius of 64 km. The T159 spectral truncation on the sphere which is used, gives an equivalent grid spacing on the corresponding reduced Gaussian grid of about 1.25 km. The study focusses on convective circulations triggered by local heating above the surface.

4.1 Constant heating

In a first set of experiments, the operational physics is switched off. It is replaced by a constant heating rate Q with a Gaussian shape (horizontal radius of 5 km, vertical depth 100 m) applied for the first 15 minutes of simulation. Then, the model runs adiabatically a further 45 minutes.

With a time step of 0.1 s, the system with the compressible coupling resolves the propagation of fast elastic waves (figure (2), red curves) which are triggered by the diabatism. These waves are not present when the "anelastic" coupling is used (figure (2), blue curves). When the heating stops, the two solutions start to converge toward each other and after one hour the NH pressure departure field is identical in the two simulations.

With a time step of 10 s, the fast short waves are not resolved anymore when the compressible coupling is used (figure (3)). The simulation with the anelastic coupling gives the same results with a time step of 10 s and with a time step of 0.1 s.

The temperature profiles in the middle of the warm "bubble" shown on figure (4) are only marginally affected by the time step. They are also almost identical in the two NH runs and the hydrostatic run at the end of the warming period. After one hour, the two NH solutions are still identical, but the hydrostatic run gives a different solution for the adjustment to the initial warming.

Simulations with a time step of 100 s give similar results to simulations with a 10 s time step.

4.2 Interpretation

A comparison of the temperature tendencies computed in the explicit part of the dynamics before the physics and in the physics (in this case reduced to a constant warming) is shown in figure (5). In the case of the compressible coupling, the negative tendency (cooling) coming from the dynamics almost

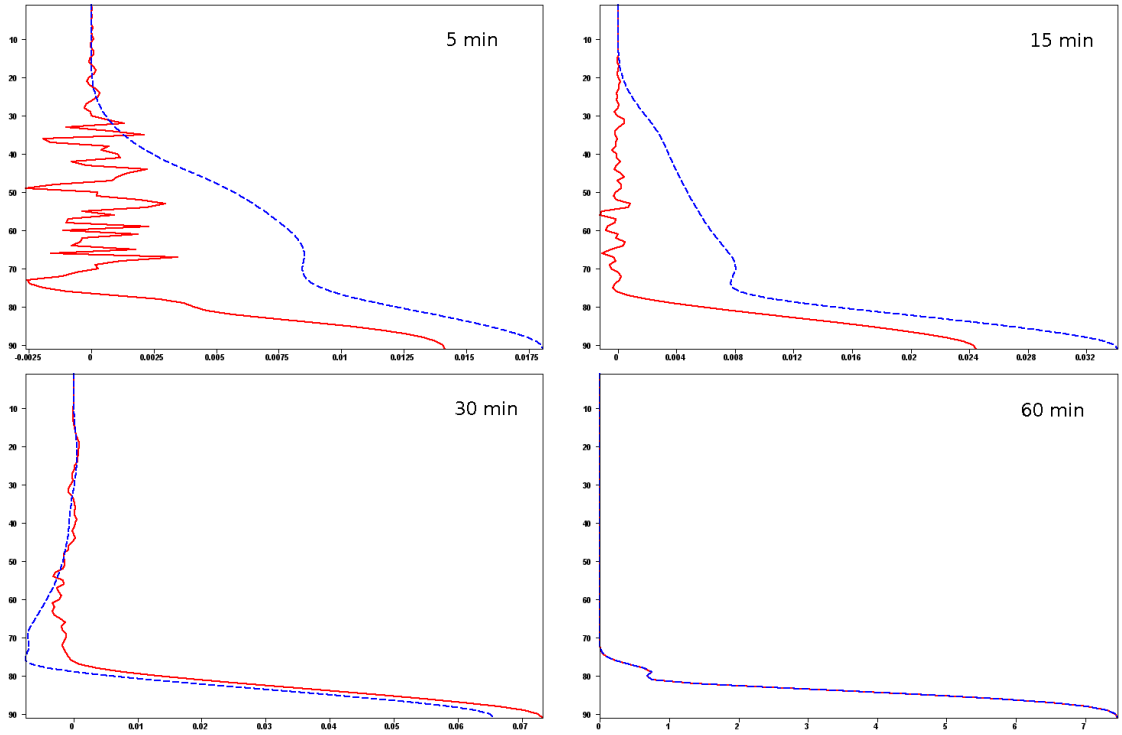

Figure 2: Vertical profiles (vertical axis shows model level indexes) of NH pressure departure in the centre of the warming after 5,15,30 and 60 min. Results for compressible (red) and anelastic (dashed blue) couplings for forecasts with a time step of 0.1 s.

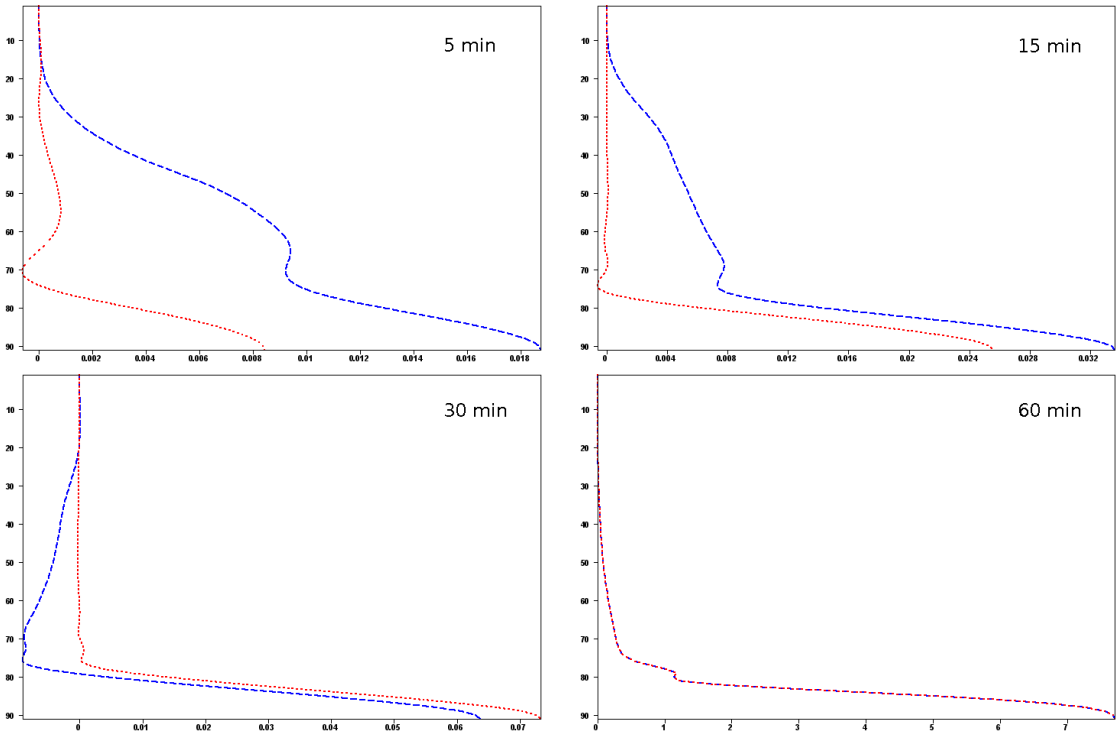

Figure 3: Vertical profiles of NH pressure departure in the centre of the warming after 5,15,30 and 60 min. Results are shown for compressible (red) and anelastic (dashed blue) couplings and for a time step of 10 s.

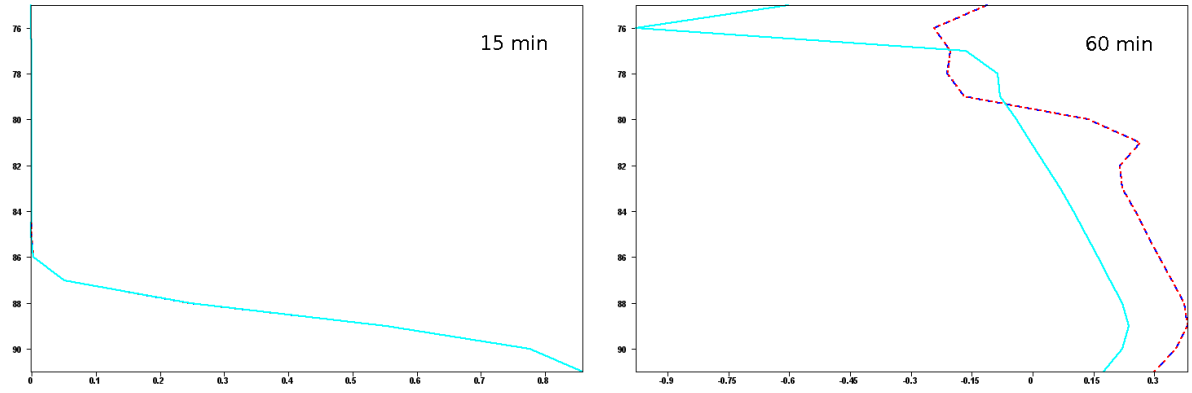

Figure 4: Vertical profiles of temperature in the centre of the warming after 15 and 60 min. Results are shown for compressible (red), anelastic (dashed blue) couplings and for the hydrostatic simulation (cyan) (results are the same for time steps of 0.1 s and 10 s).

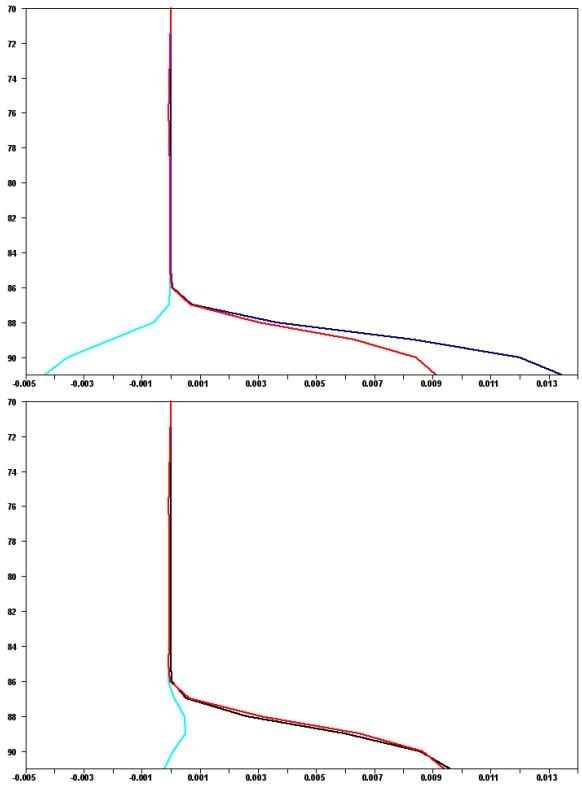

Figure 5: Vertical profiles of T-tendencies. Dynamics tendencies (cyan), physical tendencies (black) and their sum (red) for compressible coupling (top) and anelastic coupling (bottom).

exactly compensates the extra heating caused by the difference between the diabatic tendency Q/c_v of the "compressible" coupling and the diabatic tendency of the anelastic coupling Q/c_p.

In the compressible coupling, the diabatic forcing of the NH pressure departure

$$\frac{\partial_\varphi \hat{q}}{\partial t} = \frac{Q}{c_v T} \tag{8}$$

seems to be fully converted in the dynamics into a volume change (expansion if $Q > 0$)

$$\hat{D}_3 = \frac{c_v}{c_p}\frac{\partial_\varphi \hat{q}}{\partial t} \tag{9}$$

This contribution to D_3 is seen at the next time step as an adiabatic cooling in the T-equation (5) (if $Q > 0$) which, using equations (9) and (8), can be shown to be exactly equal to the difference between the heating rates Q/c_v and Q/c_p

$$-\frac{RT}{c_v}\hat{D}_3 = \frac{Q}{c_p} - \frac{Q}{c_v}$$

The residual volume change $D_3 - \hat{D}_3$ in equation (5) is associated with the volume change resulting from the more global mass re-organisation computed by the NH dynamics solver.

In the case of the anelastic coupling, the expansion of the volume following the diabatic heating is not computed in the dynamics. It is supposed to be an "instantaneous" process (process much faster than the time step, not resolved by the time step). In the approximated version of the diabatic equations (6), the air parcels never experience the extra heating and the compensating extra expansion described by the fully compressible coupling, but only the residual heating Q/c_p and the residual volume change (the

work of the NH pressure departure has already been taken into account and the temperature has been adjusted in consequence).

4.3 Adjustment to saturation

In a second series of tests, a simplified parametrisation of the adjustment to saturation has been added to the constant heating. The condensation/evaporation scheme introduces some feedback between the dynamics and the physics but it remains a reversible process (the total enthalpy of the multiphase system is conserved, no precipitation).

The same constant heating as in section 4.1 triggers adiabatic ascents. The condensation starts after about one hour and then moist convection starts and a deep cloud is formed.

The condensation scheme returns T-tendencies which may be used within an "anelastic" coupling or a "compressible" coupling as explained in section 2.4.

The computation of the supersaturation in the parametrisation of the adjustement to saturation is an iterative procedure which finds the correct equilibrium between the water phases and the temperature (the adjusted temperature depends on the condensation rates, but the condensation rate depends on the saturation mixing ratio which depends on the temperature).

The evolution of the temperature due to latent heat release in the iterative algorithm of the condensation scheme cannot be solved by the complete compressible system of equations because of the hypotheses inherent in the physics. A usual hypothesis is to suppose that the condensation heats the air in the grid box at constant pressure. The increment of the temperature is then estimated as:

$$\Delta T = \frac{L}{c_p}\Delta q_l$$

where L is the latent heat of vaporization.

However, in the NH model with a compressible coupling, the pressure (or at least the NH pressure departure) can be modified by diabatic effects (equation (4)). As the air is supposed to be motionless in the physics computations, it is quite logical to suppose that the air in the grid box is heated at constant volume (in the fully compressible system of equations, any volume change is theoretically described by the resolved motion). In this case, the increment of the temperature in the condensation scheme is estimated as:

$$\Delta T = \frac{L}{c_v}\Delta q_l$$

In the non-hydrostatic model, the two options for the physics/dynamics coupling can be combined with the two options for the computation of the supersaturation. The three following combinations are of interest :

- Anelastic coupling with a condensation scheme at constant pressure
- Compressible coupling with a condensation scheme at constant pressure
- Compressible coupling with a condensation scheme at constant volume

For a time step of 10 s, the results of the three experiments are very similar (figure (6), left pannels). But for a time step of 100 s, the experiment with the compressible coupling and a condensation scheme at constant pressure gives significantly different results (figure (6), right pannels).

The balance reached in the physics between the water phases and the temperature is disturbed when the temperature tendency is multiplied by c_p/c_v for the compressible coupling. Even if the dynamics

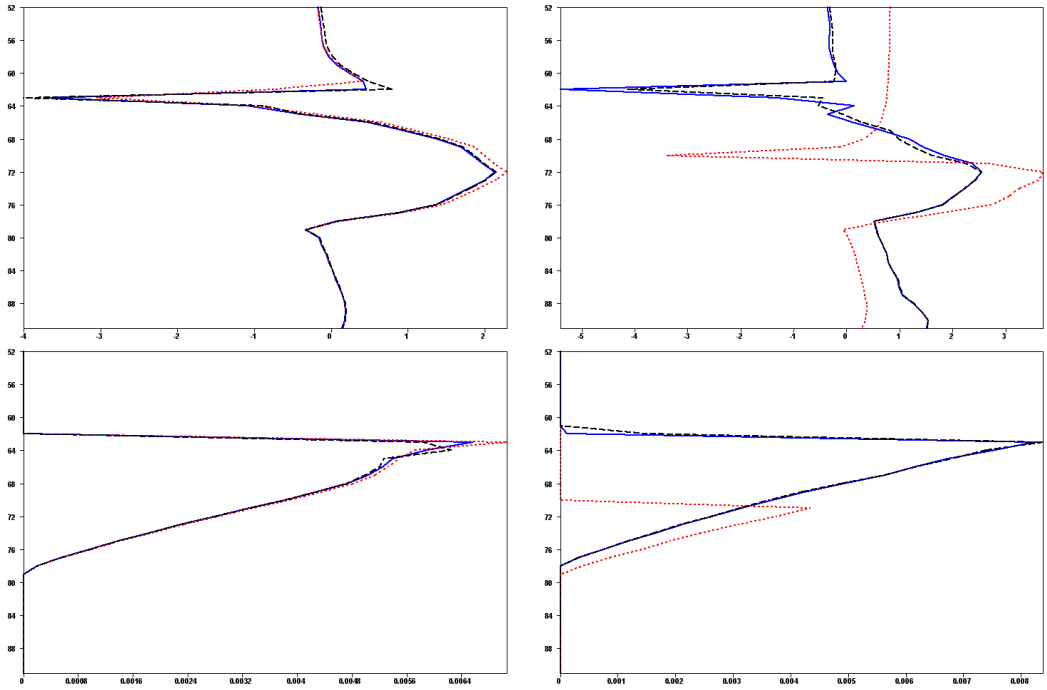

Figure 6: Vertical profiles of potential temperature (top) and cloud liquid water content (bottom) in the middle of the cloud after 85 min of simulation for time steps of 10 s (left) and 100 s (right). Results for anelastic coupling with condensation at constant pressure (blue curves), for compressible coupling with condensation at constant pressure (red curves) and for compressible coupling with condensation at constant volume (black curves).

reproject the diabatic tendency of the NH pressure departure onto the volume change at the beginning of the next time step, this inconsistency in the equations is sufficient to change the cloud simulation in the case of the long time step. Similar inconsistencies are probably at the origin of the differences between the NH simulation with the compressible coupling to the current physics (at constant pressure) and the hydrostatic simulation, which have been carried out in the hydrostatic range (section 3).

5 Conclusion

The NH dynamical core of the IFS has been validated by conventional idealised adiabatic experiments in the hydrostatic range and in the NH range using the small planet configuration (Wedi et al, 2009).

The first step of the validation of the coupling between the NH dynamical core of the IFS and diabatic processes is presented in this paper. It suggests that the physics solvers based on a "constant pressure" hypothesis can be coupled with the NH IFS dynamical core if the physics/dynamics interface also assumes an instantaneous projection of the diabatic NH pressure departure tendencies onto a volume change and the corresponding temperature adjustment. This instantaneous adjustment corresponds to an anelastic filtering of the diabatic forcing as found by Thurre et al (1998).

The following steps in the validation of the NH physics/dynamics coupling will be an analysis of the coupling with the prognostic microphysics recently developed at ECMWF and a study of the impact of the choice of "hydrostatic" conservative variables such as the static energy in the physics solvers.

References

Bubnova, R., G. Hello, P. Benard, and J.-F. Geleyn (1995). Integration of the fully elastic equations cast in the hydrostatic pressure terrain-following coordinate in the framework of the arpege/aladin NWP system. *Mon. Weather Rev. 123*, 515–535.

Thurre, C. (1998). *Etude de l'ajustement hydrostatique suite à un forçage diabatique dans un modèle pleinement élastique*. Ph. D. thesis, Cooperative Program UQAM-McGill U.

Wedi, N. P. and P. K. Smolarkiewicz (2009). A framework for testing global non-hydrostatic models. *Quart. J. Roy. Meteor. Soc. 135*, 469–484.

Wedi, N. P., K. Yessad, and A. Untch (2009). The non-hydrostatic global ifs/arpege model: model formulation and testing. Technical Memorandum 594, ECMWF. 34 pp.